Making precious metals cheap: A sonoelectrochemical – Hydrodynamic cavitation method to recycle platinum group metals from spent automotive catalysts

Eugeniu Vasile [a], Adrian Ciocanea [b,*], Viorel Ionescu [c], Ioan Lepadatu [d], Cornelia Diac [e,f], Serban N. Stamatin [e,f,*]

[a] *Department of Oxide Materials and Nanomaterials, Faculty of Applied Chemistry and Material Science, University "Politehnica" of Bucharest, Bucharest 060042, Romania*
[b] *Power Engineering Faculty Hydraulics, Hydraulic Machines, and Environmental Engineering Department, University "Politehnica" of Bucharest, Bucharest 060042, Romania*
[c] *Department of Physics and Electronics, Ovidius University of Constanta, Constanta 900527, Romania*
[d] *National R&D Institute for Optoelectronics – INOE 2000, Bucharest 077125, Romania*
[e] *3Nano-SAE Research Centre, University of Bucharest, 077125, Romania*
[f] *Faculty of Physics, University of Bucharest, 077125, Romania*

ARTICLE INFO

ABSTRACT

Platinum group metals, such as Pd and Pt, found in three-way catalyst converters were recycled in a two-step method: hydrodynamic cavitation followed by sonoelectrochemical dissolution. High shear forces were obtained by using a convergent nozzle with a throat diameter of 0.2 mm, feeded by a plunger pump at a pressure of 60 MPa. Cavitating submerged jets acted locally on the water dispersed waste catalyst. As-obtained samples were analyzed by scanning electron microscopy and transmission electron microscopy. Electron microscopy on the initial sample showed that round shaped Pd and Pt nanoparticles were randomly distributed on the Al_2O_3 matrix. Cavitated samples show two zones in which Pt and Pd were partially and completely separated from the cordierite. The hydrodynamic cavitation separates the Pd and Pt from the cordierite leading to an apparent increase in Pd and Pt concentrations of 9% and 34% respectively. Conventional electrochemistry showed a dissolution of 20% in 1 h. To further accelerate the dissolution, a sonotrode operating at 20 kHz and 75 W was placed inside an electrochemical cell in order to increase the mass transport and obtain high dissolution rates. Indeed, the results showed that 40% of the available Pd and Pt can be recycled in just 1 h. In the absence of hydrodynamic cavitation and using conventional electrochemistry less than 10% of the available Pt and Pd is recovered in 1 h. The cost analysis showed that Pd and Pt can be recovered at less than 10 EUR per g which is 5 times smaller than their current market price.

1. Introduction

Modern emission control systems inside every vehicle are based on the Three-Way Catalyst (TWC) converter, which reduces NOx and oxidizes all unused hydrocarbons and carbon monoxide. The common car catalytic converters are incorporating a honeycomb type cordierite skeleton ($Mg_2Al_4Si_5O_{18}$) as the substrate. A large contact area for the catalytic processes is created by coating the inner surface of the skeleton with a washcoat of 50–100 μm thickness. A highly doped porous γ - Al_2O_3 is used as a washcoat. Common dopants to stabilize catalytic converters are Ce, Zr, La, Ti and alkaline-earths [1].

Active components in the washcoat are based on ultra-fine Platinum – Group Metals (PGMs): platinum (Pt), palladium (Pd) and rhodium (Rh) which are used as the reduction (Pt, Rh) and oxidation (Pt, Pd) catalysts. Nanoparticles of Pd and Pt are deposited on the surface of the washcoat surface [1]. PGM concentrations varies with manufacturer. In new car

catalytic converters, Pt ranges in concentration from 300 to 1000 mg/kg, Pd concentration varies from 200 to 800 mg/kg and for Rh, concentration varies from 50 to 100 mg/kg [1]. The full experimental protocol is challenging to obtain due to intellectual property rights.

PGMs are widely used in various industries which makes the PGM concentration in various wastes larger than natural ores [2]. Large scale PGM recycling is based mainly on hydrometallurgical and pyrometallurgical methods. Hydrometallurgy techniques imply pressurized cyanidation, carrier dissolution, and the total dissolution of PGM species from a spent TWC converter [3]. PGMs inertness require large amounts of strong acids and powerful oxidants which creates a large environmental footprint. The large amounts of chemicals and energy used in PGM recycling acted as the catalyst in developing alternative recycling routes, such as: two-step microwave-assisted leaching [4,5]; bio-hydrometallurgical processes [6,7]; pyrometallurgy [8–10]. The above-mentioned technologies used for PGM extraction are economically viable only in large recycling facilities. Future industries that are large energy consumers, large CO_2 producers and environmental polluters will be restricted considerably in order to answer the environmental concerns of tomorrow. Technologies that make use of cheap renewable electricity will be favored.

The low concentration of PGM in the initial waste hinders many recycling technologies which pushed the research towards an initial separation step. W. Kim et al. [11] proposed an innovative method for the selective recovering of PGMs which was based on the physical impact/shearing action between catalyst particles and either the liquid phase or the walls in the mixing vessel [12,13]. A dislocation phenomenon of the catalyst layers from the supporting matrix is produced at the point of impact and the catalyst layer breaks under further impacts [11]. Therefore, concentrating the PGM in the initial waste is possible in a preparatory stage. The end-result of the treatment is expected to contain mostly the alumina washcoat covered with the PGM, although it is still elusive.

The use of hydrodynamic cavitation (HDC) techniques is based on the energy released by the collapse of micrometer bubbles dispersed in the liquid. It has been shown that HDC generate a chemical effect (e.g. production of radical active species) and a mechanical effect (e.g. turbulence, shear stresses) that can be used for wastewater treatment [14,15] and water disinfection [16,17]. Submerged cavitating jet under different operating conditions proved to be an efficient tool for metal surface erosion at the nano-level with the possibility of using the cavitation bubbles as a nanofabrication method [18]. In this respect, the bubble resulted from HDC generates sufficient mechanical energy for it to serve as a pretreatment stage of the automotive catalyst in which the PGM containing layer can be removed effectively from the major component, that is cordierite.

PGM recovery from alumina supports has been tackled before in the literature. Most of the techniques are based on the recovery of PGMs using concentrated HCl (>3 M), moderate temperatures (>80 °C) [19,20] or even HCl-H_2O_2 mixtures [21]. Other methods are based on treating the alumina in a 6 M H_2SO_4 at 100 °C with a dissolution time of 2 – 4 h [22]. Approximately 50% of the PGM were electrochemically recycled in 24 h from an automotive catalyst [23]. The bottleneck in PGM recovery is the mass transfer of reactants and products to and from the electrode. Turbulent flow, cavitation and microjets are well-known phenomena caused by ultrasounds that can alter the Nernst diffusion layer [24]. Indeed, it was shown that the transport limiting current increases fivefold when an ultrasonic horn is used [25,26]. In this respect, sonoelectrochemical synthesis of nanometric Pt from aqueous based Pt chlorides under ultrasonic irradiation has received increasing attention in the past decade [27,28]. However, reports on the sonoelectrochemical recovery of metals are very scarce in the literature [29,30] in spite of the increased mass transport that stimulates the dissolution rate.

Electrochemical recovery of PGMs from spent automotive catalysts based on the Pt-$[PtCl_6]^{2-}$ redox couple has been shown in our recent

study [23] which resulted in a dissolution rate of less than 50% in 24 h. The small PGM concentration in the initial automotive catalyst and poor mass transfer were found to hinder the overall dissolution rate. Herein, we made use of hydrodynamic cavitation to increase the PGM concentration and coupled it to a sonoelectrochemical PGM dissolution in order enhance the mass transport. The results show that the hydrodynamic cavitation acts as a PGM concentrator in the catalyst by removing the cordierite that does not contain PGM, resulting in a PGM concentration increase. Furthermore, a sonoelectrochemical treatment is applied on the catalyst. The total recycling time is reduced by a factor of 20 compared to our previous results [23].

2. Experimental

2.1. Materials

Hydrochloric acid (HCl, 37%) was purchased from Lachner (Czech Republic). Ultrapure water (>18.2MΩ*cm) was supplied by a Milli-Q Direct Q System (Burlington, MA, U.S.A.). Multi-element Calibration Standard 4 (PerkinElmer, Inc., U.S.A.) was used to construct a calibration curve.

2.2. Catalyst pretreatment

The active materials containing noble metals were collected from the monolith substrate of the used gasoline catalyst converter supplied by a local scrap metal shop. A preliminary selective powdering, using a scalpel for the material scrapping was initially accomplished. A mechanical processing stage of the powder was performed after, for an enhanced homogenization of the samples investigated microscopically. The powder was processed by a laboratory milling system, based on a container in which rotors with teeth are placed. An interstice of up to 0.3 – 0.5 mm was calibrated between the rotor surface and the bottom of the collecting vessel.

2.3. Hydrodynamic cavitation method

Hydrodynamic cavitation was used as a mechanical method for destructuration of a TWC spent catalyst fractured, milled and dispersed in distilled water inside a cavitation chamber. A cavitation system was designed and manufactured as presented in Fig. 1A. An upstream pressure of 60 MPa obtained by using a plunger pump (PP) is acting on a convergent nozzle with a throat diameter of 0.2 mm (Fig. 1B). A constant flow rate of 0.469 L/min was maintained during the cavitation process. Because the flow discharged by the plunger pump (PP) increases the level in the storage chamber (3.2) the dimensions of the cavitation chamber (3.1) was settled down at a minimum volume for recirculation purpose of the milled powder dispersed in distilled water in the action area of the submerged cavitation jet. For the design of cavitation chamber, a separate study was performed for identifying the dimensions of the submerged jet considering the working conditions, as presented in Fig. 1C [31]. The results of this study are in line with other research that cover the subject of the length of the cavitation submerged jets [32,33].

Three rounds of hydrodynamic cavitation were performed each of them consisting in producing of about 50 submerged jets generated in the cavitation chamber. A volume of 1.5 L of biphasic fluid was obtained at the end of each round. The sediment obtained after one cavitation round was introduced in the cavitation chamber for another round at the same parameters. Therefore, the particles of spent catalyst were subjected to 150 cycles of hydrodynamic cavitation.

When the submerged jet penetrates the relatively stagnant distilled water containing dispersed catalyst particles inside the cavitation chamber, high shearing forces are generated. The exchange of momentum from one region of the fluid to another region as the result of high values of jet velocity generate intense shear stress. At the micro
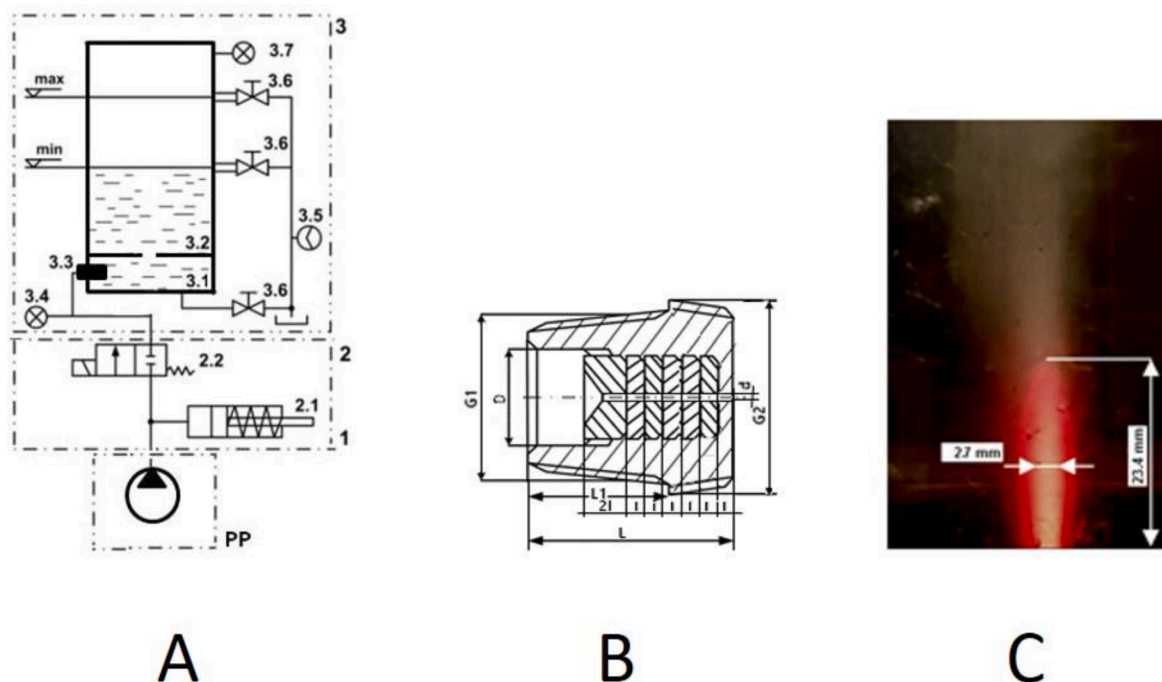
Fig. 1. (a) Cavitation jet system (PP - Plunger pump; 2 - Pressure distribution system: 2.1 - Accumulator, 2.2 - Electric distributer; 3 – Installation: 3.1 – Cavitation chamber, 3.2 Storage chamber, 3.3- Nozzle, 3.4 - Low pressure transducer, 3.5 - Flow indicator, 3.6 - Valve, 3.7 - High pressure transducer); (b) Cavitation nozzle (d = 0.2 mm, l = 1 mm); (c) Geometric characteristics (2.7 mm width and 23.4 mm height) of the submerged jet for an upstream pressure of 60 MPa.

level when cavitation bubbles from the cloud hit a particle a plastic deformation occur. Also, the small space between bubbles accelerate the fluid, generating micro-jets which are increasing kinetic energy and creates shockwaves [34]. Some research reported that the maximum jet velocities are between 50 and 100 m/s [35] or even more, i.e. 950 m/s near an elastic boundary [36]. Also, the pressure values coresponding to the local material stress induced by the micro-jets varies between 100 to over 1000 MPa [37]. As a result, erosion may occur which removes material from the particles surface therefore exposing aluminum oxide layers by erasing the surface of cordierite matrix.

2.4. Sonoelectrochemical method

2.4.1. Electrode preparation

The experimental setup consists of three electrodes connected to a potentiostat (OrigaFlex – OGF500) which is controlled by OrigaView software. The horn of an ultrasonic processor (Ultrasonics, FS – 250 N) was placed between the working and counter electrode. Titanium plates were used as working electrode (approx. 2.80 cm^2) and counter electrode (11.31 cm^2). The working electrode was sprayed with an homogenized aqueous solution of 0.2 g spent catalyst powder or HDC treated sample. The catalyst was milled and mixed with 5 mL 1 M HCl for 30 min. The mass of catalyst was estimated by weighing the plate before and after deposition. Ag/AgCl was used as reference electrode with a measured potential of 199.8 ± 0.3 mV vs. SHE Supplementary Information. All potentials were referenced against the standard hydrogen electrode (SHE). The electrolyte solution was 1 M HCl prepared from concentrated HCl (35%) and diluted in ultrapure water (>18.2MΩ*cm). The working electrode was sprayed with an homogenized aqueous solution of 0.2 g spent catalyst powder Supplementary Material. An airbrush connected to an air compressor (AF186 Mini Air Compressor – Piston Type) was used for spraying Supplementary Material. The deposition was made on a hot plate. ICP – OES (Perkin Elmer, Avio 200, USA) was used to determine the amount of platinum dissolved.

2.4.2. Potential of the reference electrode

Ag/AgCl was used as reference electrode with a measured potential of 199.8 ± 0.3 mV vs. SHE. The potential of the reference electrode was measured with an electrochemical cell with two platinum electrodes and the electrolyte solution (1 M HCl). The electrolyte solution was purged with hydrogen (Hydrogen generator, Perkin Elmer – PGKH$_2$ 500) continuously throughout the measurements. Further details on the measurement can be found in [23]. The obtained potential was 199.8 ± 0.3 mV

2.4.3. Electrochemical procedure

Chronoamperometry – potential step was used as electrochemical method and recorded for 60 min. First step (minimum potential) was set at 0.25 V vs. Ag/AgCl and the second step (named maximum potential) was set at 1.15 V vs. Ag/AgCl. The step duration was set at 0.02 s. For sonoelectrochemistry we used a sonotrode controlled by an ultrasonic processor. A 1 s ON and 1 s OFF ultrasound profile was performed for 60 min. The temperature in the electrochemical assembly was maintained below 15 °C throughout the experiments by means of an ice bath.

2.5. Nanoscale characterization

A scanning electron microscope (SEM) Quanta Inspect F (FEI-Philips) working at an acceleration voltage up to 30 kV and equipped with energy dispersion X-rays spectrometer detector (EDAX^R with a 132 eV resolution at Mn Kα) was used to determine surface morphology and elemental composition of different samples of a gasoline catalyst waste powder. SEM samples have been dispersed on a conducting amorphous carbon tape and attached to an aluminum holder.

A transmission electron microscope (TEM) model Tecnai G^2 F30 S-Twin, (FEI-Philips) operated at an acceleration voltage of 300 keV and equipped with an X-ray energy dispersive spectroscopy (EDAX^R System) was used to investigate the microstructure, composition and crystallographic phases of nanometric sized crystalline agglomerates obtained after the HDC processing of automotive waste powder. Preparation of the TEM samples involved an ultrasonic dispersion of the catalyst waste

powder in ethanol, with one drop of the suspension placed after onto a copper grid covered with a holey amorphous carbon film.

3. Results and discussions

Automotive catalysts are overly complex structures formed of a cordierite backbone on which a washcoat is deposited. The waschoat is usually a mix of Al, Ce, Zr and Ti oxides depending on the type of catalyst (gasoline or diesel) as well as the manufacturing year. Catalytic active nanoparticles, such as Pt and Pd, are usually deposited on the washcoat. A mechanical pretreatment of the catalyst was used to obtain a powder with uniform particles (see Experimental Supplementary Material).

3.1. Metal concentration before and after hydrodynamic cavitation

Platinum group metal (PGM) concentration in the spent catalyst powder was measured by inductively coupled plasma-optical emission spectrometry (ICP-OES Supplementary Material The Pt concentration was determined to be (0.135 ± 0.003) g Pt per kg corresponding to 0.014% Pt. The Pd concentration was determined to be (0.447 ± 0.025) g Pd per kg corresponding to 0.045% Pd. The automotive catalyst composition presented herein was similar to our previous article [25].

Pt and Pd concentration in the sediment and liquid was determined by ICP-OES (Table 1). There was no Pt and Pd detected in the liquid. However, the liquid turned opaque after the cavitation which suggests that mostly cordierite was dispersed in the solution. The PGM concentration in the sediment increased by 34% and 9% for Pt and Pd, respectively. The shock-waves produced by cavitation separates the washcoat from the cordierite which results in an increase in the PGM concentration. An advanced nanoscale characterization was carried out in order to elucidate the cavitation effect on the morphology and structure of the catalyst.

3.2. Nanoscale characterization of the pristine automotive catalyst

The sample was initially characterized by Backscattered Electron Imaging (BSEI) SEM (Fig. 2). The reader should bear in mind that the brightness in BSEI SEM is governed by the atomic number: higher average atomic numbers are brighter than lower average atomic numbers. The BSEI technique, combined with the EDX technique can assist in lateral resolution to identify nanometer-sized particles through atomic number contrast [38]. Agglomerates of uniform grey color, having different shapes and orientations and minimum dimensions of a few microns could be observed in the BSEI image. An agglomerate of a few dozen bright nano-spots, with diameter between 10 and 30 nm, were identified at the surface of one micrometrical structure (see the inset image in Fig. 2).

The surface elemental composition for the SEM micro-structure containing nano-spots was determined through energy dispersion X-rays spectrometry (EDX). Two regions were selected: *zone 1* of uniform grey contrast and *zone 2* incorporating most of the bright nano-spots (see the inset image in Fig. 2). EDX spectrum generated from zone 1 indicated the presence of some elements forming different oxides inside the spent catalyst powder: Mg and Si from the cordierite matrix; Al, present both in cordierite and washcoat structures; Ti from the washcoat layer. Small traces of Pt and Pd could be detected here, through only one M and L X-ray emission line, respectively. The existence of Ca in the spectra

was associated with possible contamination from engine oil [39]. Iron was also found in the spectra which can be considered here as a catalyst converter contaminant or a secondary dopant in the cordierite. EDX investigation of zone 2 revealed the clear presence of Pd and Pt through different X-ray emission lines, along with all the elements identified also in zone 1.

The Bright – Field Transmission Electron Microscopy, hereinafter TEM, analysis showed the co-existence of alumina layers with different thickness covering portions of the cordierite matrix (Fig. 2B). Round, darker nano-spots of various diameters were found on thin alumina layers which were associated with Pd and Pt (*vide-infra*). EDX measured on one nanoparticle (see the inset image in Fig. 2B) confirmed the presence of Pt using the X-ray Mα line at 2.047 keV, Lα line at 9.41 keV and Lβ line at 11.13 keV. The existence of Pd was established through the strongest X-ray Lα line at 2.839 keV, Kα line at 21.14 keV and Kβ line at 23.805 keV. No ruthenium X-ray Lα peak (at 2.696 keV) was identified in this investigated nano-area. A similar observation was reported from another EDX study regarding the elemental Rh presence in gasoline type spent catalyst [40]. Pd and Pt content is five to ten times greater than Rh content in gasoline catalysts [41–44] which makes it challenging to identify Rh through various spectroscopy analyses. Aluminum from the Al_2O_3 coating layer and small traces of Si from the cordierite substrate were also identified in this EDX spectrum. The strong Cu peaks present here are produced by the TEM sample grid.

The catalyst under investigation showed a complex structure formed of a cordierite backbone on which a washcoat is deposited. PGMs were found on the washcoat surface. To increase the PGM recovery rate, the washcoat with the PGM should be separated from the cordierite. The separation degree of PGMs from the washcoat layer and from the cordierite matrix is investigated in the following. The washcoat layer consisted of Al, Ce, Zr, Ti and La oxides. At the end of the cavitation, the sediment separated into two distinct colored sediments (light grey and dark grey) which were further analyzed by SEM and TEM. The electron microscopy investigations show a partial and a complete isolation of the washcoat in the light grey and dark grey areas, respectively.

3.3. Partial separation of the washcoat from the cordierite

A few dozen bright nano-spots could be observed in the SEM - BSEI image of the light grey sediment (Fig. 3A). The nanospots were closely – packed or isolated on a uniform grey matrix. EDX analysis performed on a nano-region with agglomerated spots of different sizes indicated the presence of Pt and Pd (Fig. 3A). Small traces of La and Fe from the washcoat layer were determined as well. There were no homogeneous mixtures of the washcoat and cordierite as shown in Fig. 2B.

The washcoat was found to be partially attached to the cordierite, throughout the whole investigation of this area (Fig. 3B). TEM images (Fig. 3B) showed the presence of a thin alumina layer containing uniformly distributed Pd and Pt nanoparticles. EDX investigations along a uniform grey nano-region revealed the presence of cordierite (EDX 1, Fig. 3B). A light grey region including a dark spherical nanocrystal of about 60 nm in diameter (EDX 2, Fig. 3B) confirmed the presence of Pt, Pd and Al. Additional electron microscopy investigations that support the separation from the cordierite are presented in Figure S1 (see Supplementary Material). The strong Fe and Co peaks located at 6.40 and 6.93 keV, respectively, were generated from the TEM specimen chamber or contaminants from the engine, cordierite or even sample preparation. However, the origin of Fe and Co falls beyond the scope of this work.

3.4. Sonoelectrochemical recycling of PGM

The automotive catalyst is a complex structure that contains several electrochemically active components. A polycrystalline Pt disc electrode was used initially to emphasize the role of the ultrasound on the dissolution rate and to develop a sonoelectrochemical protocol. Pt is less prone to electrochemical corrosion than Pd [45] and it was expected for

Table 1
Summary of the Pt and Pd concentration before and after the cavitation.

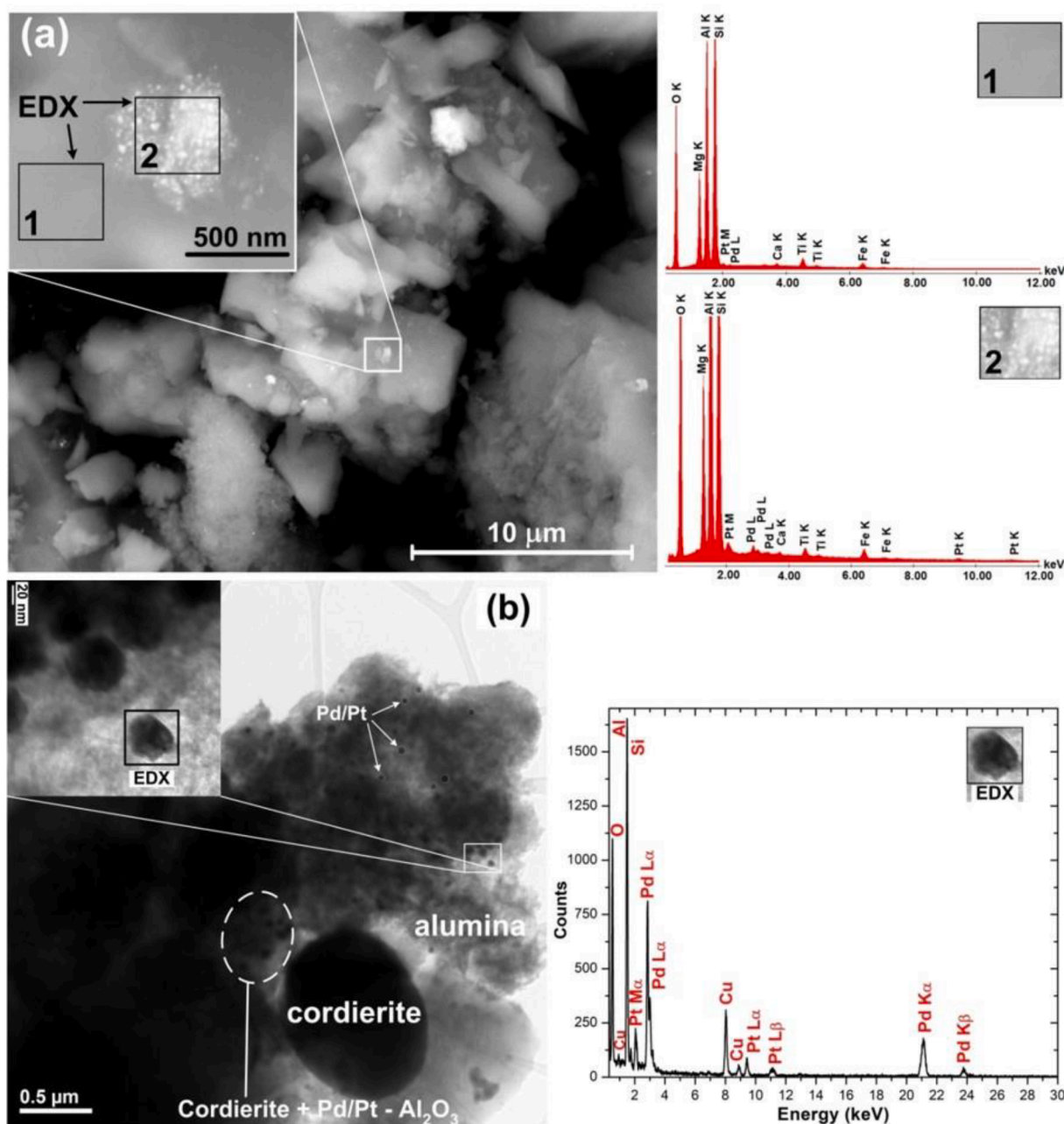|	Initial (mg/kg)	After hydrodynamic cavitation		Efficiency
		sediment (mg/kg)	liquid (mg/l)	
Pt	135	178	0	+34%
Pd	447	487	0	+9%

Fig. 2. (a) SEM - BSEI micrographs and (b) BF-TEM images of samples before hydrodynamic cavitation treatment, along with some specific EDX spectra generated from different regions.

Pd to show a dissolution rate at least equal to that of Pt. Fig. 4A shows the ultrasound effect on the dissolution rate. Conventional electrochemistry, that is a regular steady-state electrochemistry in a 3-electrode geometry, resulted in consistently smaller dissolution rates than the sonoelectrochemical route. A flattening behavior was observed after 2 h for the conventional method which can be reasoned on the poor mass transport in steady-state electrochemistry. The reader should bear in mind that the dissolution rate of conventional electrochemistry without hydrodynamic cavitation is similar to the previously reported value by our groups [23]. The sonoelectrochemical procedure showed a steady increase in the dissolution rate. It is well-known that the ultrasounds are increasing the diffusion of species to and from the electrode which can explain the continuous increase in the dissolution rate [26].

The role of the ultrasound profile was investigated in Fig. 4B which shows three different measurements: (1) the ultrasound is generated when 1.35 V vs. RHE is applied at the working electrode – 3sec On/Off; (2) the ultrasound is generated at 0.45 V vs. RHE – 3 sec Off/On and (3) the ultrasound is generated for 1 electrochemical cycle and turned off for the next cycle. The experiments took place in an identical electrochemical setup. The differences in the Pt dissolution among these tests were found to be less than 10% which indicated that there was no relation between the ultrasound and the type of reaction at the working electrode, that is reduction or oxidation.

We made use of the knowledge developed herein and applied it to the automotive catalyst after the hydrodynamic cavitation. The catalyst film is stable up to 36 h on the Ti plates. There was no Pt and Pd detected in the final solution when the ultrasound generator was on and the potentiostat was turned off. The experiments were set to 1 h in order to make sure that there is no catalyst falling off the electrode.

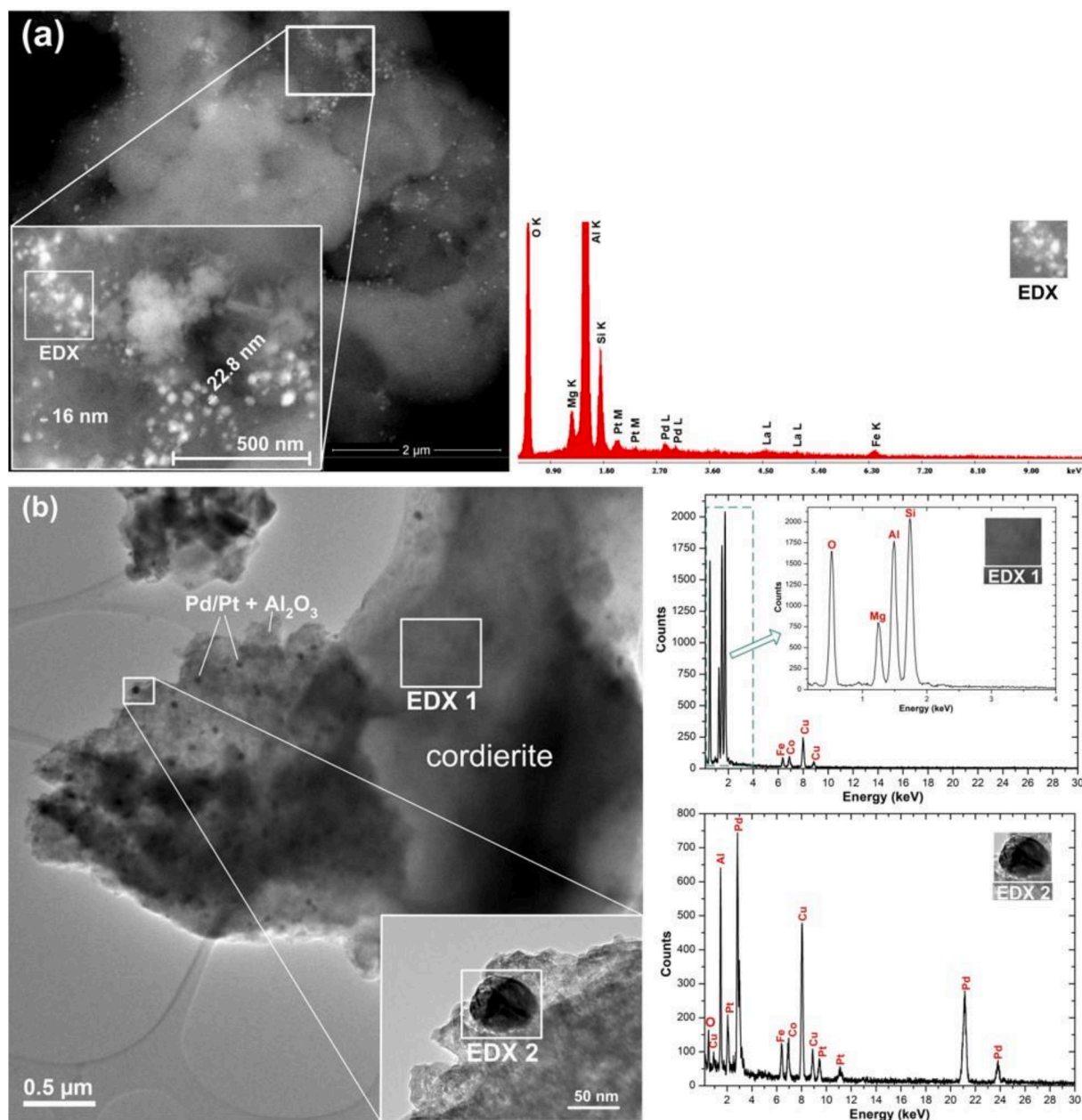The catalyst is identical to the one used in our previous study where a

Fig. 3. SEM - BSEI micrograph (a) and TEM image (b) of a sample collected from the light-grey *sediment* of the catalyst waste precipitate, obtained after HDC processing, along with the corresponding EDX spectra generated from different nano-regions.

total recycling efficiency of 47.9% was achieved in 24 h for Pt and Pd combined [23]. The hydrodynamic cavitated catalyst was subjected to conventional electrochemistry which resulted in less than 20% recovery during 1 h. The same cavitated catalyst following sonoelectrochemical recycling resulted in an efficiency of 40.6% for Pt and Pd, respectively, in 1 h. The reader should bear in mind that the previous dissolution of 47.9% was achieved in **24 h** without a hydrodynamic cavitation step [23], while, sonoelectrochemical coupled hydrodynamic cavitation showed a 40.6% dissolution in **1 h**. It is challenging to distinguish between metal nanoparticles and metal ions on the sole basis of ICP-OES. UV–Vis is a well-known technique to identify specific Pt aqueous chlorides [46] which was used herein to show that PGMs were converted to their aqueous based chlorides (see Supplementary Materials). We showed in our previous work that Pt nanoparticles from catalytic converters were converted to aqueous $[PtCl_6]^{2-}$ on the UV–Vis [23].

All in all, we showed that the HDC treatment of the pristine automotive catalyst removes the cordierite by partially separating the washcoat from the cordierite. The HDC effect on the catalyst can be quantified by the increase in Pt and Pd concentration which can be explained only on the basis of cordierite removal. The shear stresses that takes place during HDC separates the PGM containing washcoat from the cordierite leaving a powder which has a higher PGM concentration. HDC treatment of automotive catalysts (e.g. tungsten-titanium-vanadium oxide class) has been shown recently to remove the cordierite from the washcoat and produce photoelectrocatalysts [48]. However, the HDC treatment cannot be used to recover PGM as HDC does not change the PGM chemistry, that is Pt and Pd are still in the form of metallic nanoparticles. Pt chlorides have been previously obtained electrochemically from a Pt wire [46] or from spent automotive catalysts with a 47.9% yield in **24 h** [23]. The mass transport limitation has been identified as the root-cause for the low yield [23]. Mass transport limitations under ultrasonic conditions has been thoroughly studied by the groups of Pollet [25,26] and it is generally accepted that a fivefold improvement in mass transport is achievable. Our approach to use HDC
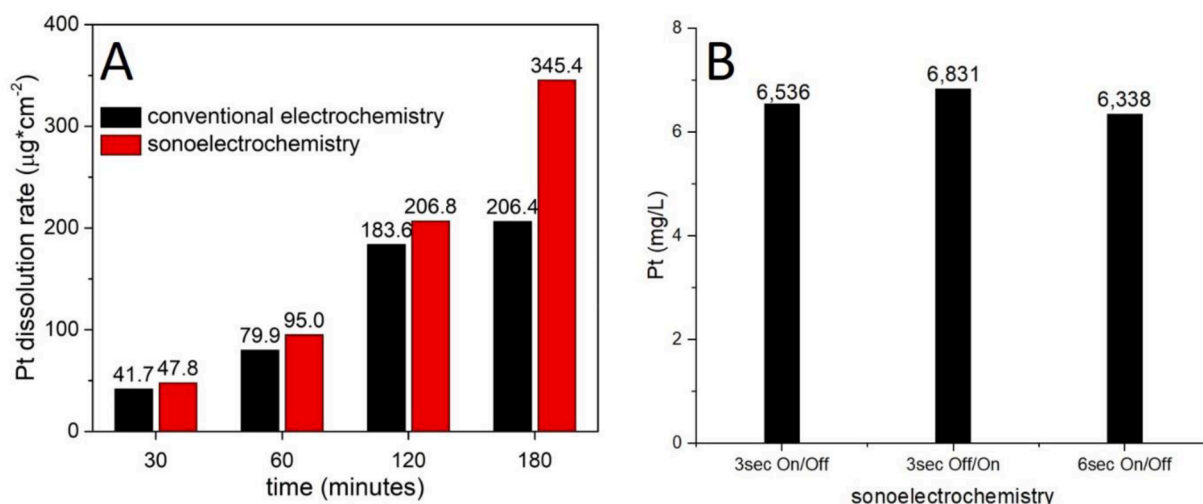
Fig. 4. (A) Conventional and sonoelectrochemical dissolution rates of Pt electrodes and (B) 3 sec on/off – ultrasound generator is turned on the upper potential; 3 sec off/on – ultrasound generator is turned on the lower potential; 6 sec on/off – ultrasound generator is turned on an electrochemical cycle and then turned off the following cycle.

as a pretreatment on the pristine automotive catalysts to increase the PGM concentration and coupling it to the faster mass transport of sonoelectrochemistry showed a 40% dissolution efficiency in **1 h**. To further show the synergistic effect of HDC and sonoelectrochemistry, a comparison between the methods is given below.

3.4.1. Comparison of the sonoelectrochemical coupled hydrodynamic method with traditional methods

The energy consumed by the system used herein is the sum of the energies consumed by the plunger pump, the ultrasound processor and the electrochemical cell. The power consumed by the plunger pump measured at the terminals of the electric motor was $P_c = 2.3$ kW for a flow rate of 0.469 L min^{-1} and an usable mechanical work of 60 MPa. The overall time for the three rounds of hydraulic cavitation was 9 min and the total energy consumed for the process was 0.35 kWh. The energy of the ultrasound processor at 1 MHz is 150 W which was used for half an hour, adding up to 0.15 kWh. The maximum current measured during electrochemistry was 0.01 mA ($=10^{-5}$ A) for 3.97 mg of catalyst. Assuming a maximum of 10 V between the working and the counter electrode, then the energy consumed in an hour for 3.97 mg of catalyst is equal to 1 mWh. However, the current increases linear with the mass of the catalyst and therefore the energy expenditure.

The total energy expenditure was computed in Fig. 5 based on the efficiency from Table 2 and the estimated energy consumption for each method (*vide-supra*). Fig. 5 compares the average price of Pt and Pd per g (dated July 25, 2020) with the methods developed in this study and our previous study [23]. Below 100 mg all the methods have a remarkably similar energy expenditure. Nevertheless, the sonoelectrochemical coupled hydrodynamic cavitation resulted in the cheapest method at about 8 EUR/g. The sonoelectrochemical method on the non-cavitated sample has an estimated cost of 12 EUR/g, that is 50% more than the previous method. The cavitated sample treated with conventional electrochemistry is at 19 EUR/g, that is 58% more than the previous method. The simple electrochemistry procedure on non-cavitated sample is the most expensive at 22 EUR/g which is 275% more expensive than the sonoelectrochemical coupled hydrodynamic cavitation method. The cost for the separation of Pt and Pd aqueous chloride complexes by liquid–liquid extraction was not considered, however it is well-established in the literature and is routinely used in laboratories around the world [47,49,50]. The cost evaluation should be viewed qualitatively for industrial scale use, however the costs will not vary by much at laboratory scale.

The obtained dissolution rates were obtained for a non-ideal material
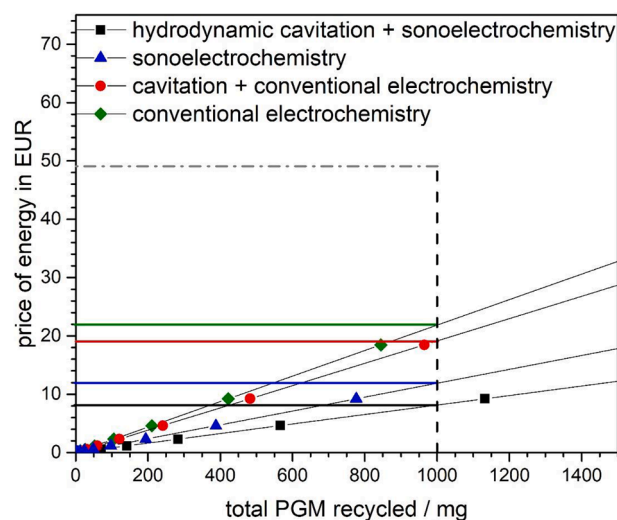
Fig. 5. Estimation of the price for PGM recycling. The vertical black dash line marks 1000 mg = 1g. Colored horizontal lines mark the prices for the energy expenditure in EUR. Grey dashed line shows the average price between Pd (67.7 EUR/g) and Pt (28.1 EUR/g), that is 47.9 EUR/g.

composite from the electrochemical point of view. The poor conduction of the alumina bottlenecks the overall process. There are many ways to further reduce the price and time of total dissolution. The most straightforward solution is to increase the size of the electrode by a factor of 20 (i.e. 2 sides of 5 cm × 5 cm = 2 × 25 cm^2 = 50 cm^2) which will most probably increase the total dissolved PGM per hour by a factor of 20 (i. e. 20 μg h^{-1}). Laboratory research on polymer electrolyte membrane fuel cells use 6.25 cm^2 electrodes at a standard 0.5 mg$_{Pt}$ cm^{-2} loading. One needs 3.5 mg of Pt including 10% losses to assemble a membrane-electrode assembly which can be produced in 175 h at 20 μg h^{-1}. Most probably in an electrochemistry group there is at least 1 potentiostat that is not used at night (5 nights × 12 h per night) and over the weekend (2 days × 24 h/day). As a result, there are at least 100 h per week when potentiostats are idle. One can obtain in 2 weeks the Pt amount needed for testing a fuel cell. At the end of the test, the Pt is in the membrane electrode assembly, an ideal material to recycle Pt. Considering a dissolution rate of 1 mg$_{Pt}$ h^{-1} (10 times that from Fig. 4) is by no means an understatement because nanoparticles are far more susceptible to

Table 2
Summary of the conventional and sonoelectrochemical recovery rates in 1 h.

	catalyst mass (μg)	beginning of experiment		end of experiment		efficiency	
		Pt(μg)	Pd(μg)	Pt(μg)	Pd(μg)	Pt(%)	Pd(%)
conventional	8410	1.49	4.09	0.26	0.70	17.1	17.4
Cavitation +sonoelectrochemical	3970	0.70	1.93	0.22	0.96	31.4	49.7

dissolution than Pt discs. To give this some context, the price of 1 g of hexahydrated H_2PtCl_6 is about 150 EUR and contains 37.5% Pt, that is 375 mg of Pt. One needs 4 weeks to obtain 375 mg of Pt at 1 mg_{Pt} h^{-1} and 100 h per week per idle potentiostat, at practically no cost. Given the extended delays in delivering chemicals that arise from the current pandemic state, electrochemistry groups around the world should consider alternative routes.

4. Conclusions

The work at-hand was aimed at finding an energy efficient and environmentally friendly solution to recycle Pd and Pt present in scrap automotive catalysts by coupling hydrodynamic cavitation and a sonoelectrochemical treatment. The hydrodynamic cavitation increased the concentration by 34% and 9% of Pd and Pt, respectively. The elemental analysis of the electrolyte before and after the sonoelectrochemical protocol showed that 40% of Pt and Pd can be recovered in just 1 h. An energy expenditure analysis was performed for each method and the results were fed into a cost-analysis. The use of hydrodynamic cavitation and sonoelectrochemistry was estimated at 8 EUR/g of Pd and Pt which is considerably smaller than the average market price of Pd and Pt (i.e. 47.9 EUR/g).

CRediT authorship contribution statement

Eugeniu Vasile: Investigation, Writing - original draft, Formal analysis, Resources. **Adrian Ciocanea:** Conceptualization, Resources, Investigation, Supervision, Writing - review & editing. **Viorel Ionescu:** Investigation, Formal analysis, Visualization, Writing - original draft. **Ioan Lepadatu:** Methodology, Investigation, Validation. **Cornelia Diac:** Methodology, Investigation, Formal analysis. **Serban N. Stamatin:** Conceptualization, Resources, Supervision, Project administration, Writing - review & editing.

Declaration of Competing Interest

The authors declare that they have no known competing financial interests or personal relationships that could have appeared to influence the work reported in this paper.

Acknowledgements

Appendix A. Supplementary data

Supplementary data to this article can be found online at https://doi.org/10.1016/j.ultsonch.2020.105404.

References

[1] D. Jimenez de Aberasturi, R. Pinedo, I. Ruiz de Larramendi, J.I. Ruiz de Larramendi, T. Rojo, Recovery by hydrometallurgical extraction of the platinum-group metals from car catalytic converters, Miner. Eng. 24 (6) (2011) 505–513, https://doi.org/10.1016/j.mineng.2010.12.009.

[2] M.K. Jha, J.C. Lee, M.S. Kim, J. Jeong, B.S. Kim, V. Kumar, Hydrometallurgical recovery/recycling of 36 platinum by the leaching of spent catalysts: A review, Hydrometallurgy 133 (2013) 23–32.

[3] K.M.N. Islam, J. Hildenbrand, M.M. Hossain, Lifecycle impacts of three-way ceramic honeycomb catalytic converter in terms of a disability-adjusted life year, J. Clean. Prod. 182 (2018) 600–615.

[4] A. Chen, S. Wang, L. Zhang, J. Peng, Optimization of the microwave roasting extraction of palladium and rhodium from spent automobile catalysts using response surface analysis, Int. J. Miner. Process. 143 (2015) 18–24, https://doi.org/10.1016/j.minpro.2015.08.007.

[5] J. Spooren, T.A. Atia, Combined microwave assisted roasting and leaching to recover platinum group metals from spent automotive catalysts, Miner. Eng. 146 (2020), 106153.

[6] D. Shin, J. Park, J. Jeong, B.-s. Kim, A biological cyanide production and accumulation system and the recovery of platinum-group metals from spent automotive catalysts by biogenic cyanide, Hydrometallurgy 158 (2015) 10–18, https://doi.org/10.1016/j.hydromet.2015.09.021.

[7] S. Karim, Y.-P. Ting, Ultrasound-assisted nitric acid pretreatment for enhanced biorecovery of platinum group metals from spent automotive catalyst, J. Cleaner Prod. 255 (2020) 120199, https://doi.org/10.1016/j.jclepro.2020.120199.

[8] F. Millo, M. Rafigh, F. Sapio, S. Wahiduzzaman, R. Dudgeon, P. Ferreri, E. Barrientos, Modeling NOx Storage and Reduction for a Diesel Automotive Catalyst Based on Synthetic Gas Bench Experiments, Ind. Eng. Chem. Res. 57 (37) (2018) 12335–12351, https://doi.org/10.1021/acs.iecr.8b01813.

[9] L.G. Zhang, Q.M. Song, Y. Liu, Z.M. Xu, Novel approach for recovery of palladium in spent catalyst from automobile by a capture technology of eutectic copper, J. Clean. Prod. 239 (2019), 118093.

[10] Y. Ding, H. Zheng, S. Zhang, B. Liu, B. Wu, Z. Jian, Highly efficient recovery of platinum, palladium, and rhodium from spent automotive catalysts via iron melting collection, Resour. Conserv. Recycl. 155 (2020), 104644.

[11] W. Kim, B. Kim, D. Choi, T. Oki, S. Kim, Selective recovery of catalyst layer from supporting matrix of ceramic-honeycomb-type automobile catalyst, J. Hazard. Mater. 183 (1-3) (2010) 29–34, https://doi.org/10.1016/j.jhazmat.2010.06.038.

[12] R. Bayley, C. Biggs, Characterization of an attrition scrubber for the removal of high molecular weight contaminants in sand, Chem. Eng. J. 111 (2005) 71–79.

[13] F. Schaaff, M. Schneider, T. Neesse, Intensifying the attrition of mineral waste in stirred mill, Int. J. Miner. Precess. 74S (2004) S291–S298.

[14] R.H. Jawale, P.R. Gogate, Novel approaches based on hydrodynamic cavitation for treatment of wastewater containing potassium thiocyanate, Ultrason. – Sonochem. 52 (2019) 214.

[15] S.M. Joshi, P.R. Gogate, Intensification of industrial wastewater treatment using hydrodynamic cavitation combined with advanced oxidation at operating capacity of 70 L, Ultrason.– Sonochem. 52 (2019) 375–381.

[16] P.R. Gogate, S. Mededovic-Thagard, D. McGuire, G. Chapas, J. Blackmon, R. Cathey, Hybrid reactor based on combined cavitation and ozonation: From concept to practical reality, Ultrason. Sonochem. 21 (2) (2014) 590–598, https://doi.org/10.1016/j.ultsonch.2013.08.016.

[17] P.R. Gogate, V.S. Sutkar, A.B. Pandit, Sonochemical reactors: Important design and scale up considerations with a special emphasis on heterogeneous systems, Chem. Eng. J. 166 (2011) 1066–1082.

[18] P.R. Gogate, A.B. Pandit, A review and assessment of hydrodynamic cavitation as a technology for the future, Ultrason. Sonochem. 12 (2005) 21.

[19] Y. Yang, L. Hu, Q. Li, B. Xu, X. Rao, T. Jiang, Recovery of Palladium from spent Pd/Al$_2$O$_3$ catalyst by hydrochloric acid leaching, Characteriz. Miner., Metals, Mater. (2016) 311–318.

[20] Y. Ding, H. Zheng, J. Li, S. Zhang, B. Liu, C. Ekberg, An Efficient Leaching of Palladium from Spent Catalysts through Oxidation with Fe(III), Materials 12 (2019) 1205–1218.

[21] Y. Ding, H. Zheng, J. Li, S. Zhang, B. Liu, C. Ekberg, Z. Jian, Recovery of Platinum from Spent Petroleum Catalysts: Optimization Using Response Surface Methodology, Metals 9 (2019) 354–373.

[22] M.S. Kim, E.Y. Kim, J. Jeong, J.C. Lee, W. Kim, Recovery of Platinum and Palladium from the Spent Petroleum Catalysts by Substrate Dissolution in Sulfuric Acid, Mater. Trans. 51 (2010) 1927–1933.

[23] C. Diac, F.I. Maxim, R. Tirca, A. Ciocanea, V. Filip, E. Vasile, S.N. Stamatin, Electrochemical Recycling of Platinum Group Metals from Spent Catalytic Converters, Metals 10 (2020) 822–833.

[24] M.H. Islam, M.T.Y. Paul, O.S. Burheim, B.G. Pollet, Recent developments in the sonoelectrochemical synthesis of nanomaterials, Ultrason. Sonochem. 59 (2019), 104711.

[25] B.G. Pollet, J.-Y. Hihn, M.-L. Doche, J.P. Lorimer, A. Mandroyan, T.J. Mason, Transport limited currents close to an ultrasonic horn: equivalent flow velocity determination, J. Electrochem. Soc. 154 (2007) E131.

[26] B.G. Pollet, The Use of Power Ultrasound for the Production of PEMFC and PEMWE Catalysts and Low-Pt Loading and High-Performing Electrodes, Catalysts 9 (2019) 246.

[27] V. Zin, B.G. Pollet, M. Dabala, Sonoelectrochemical (20 kHz) production of platinum nanoparticles from aqueous solutions, Electrochim. Acta 54 (2009) 7201–7206.

[28] B.G. Pollet, The use of ultrasound for the fabrication of fuel cell materials, Int. J. Hydrogen Energy 35 (2010) 11986–12004.

[29] B.G. Pollet, J.P. Lorimer, S.S. Phull, J.Y. Hihn, Sonoelectrochemical recovery of silver from photographic processing solutions, Ultrason. Sonochem. 7 (2000) 69–76.

[30] B. Dong, A. Fishgold, P. Lee, K. Runge, P. Deymier, M. Keswani, Sono-electrochemical recovery of metal ions from their aqueous solutions, J. Hazard. Mater. 318 (2016) 379–387.

[31] A. Ciocânea, A., Sauciuc, R., Lepădatu, I., Budea, S., Şefu, Ş.M., Simionescu, 2019 Method and demonstrating installation for recovery of titanium and tungsten oxides from spent SCR catalyst part I – scaling of hydrodynamic cavitation method, Proceedings of International Conference on Hydraulics and Pneumatics HERVEX November 2019, pag. 243–248, ISSN 1454-8003.

[32] Y. Yang, Wei Li, Weidong Shi, Wenquan Zhang, Mahmoud A. El-Emam, Numerical Investigation of a High-Pressure Submerged Jet Using a Cavitation Model Considering Effects of Shear Stress, Processes 2019, 7(8), (2019) 541.

[33] M.M. Wright, B. Epps, A. Dropkin, T.T. Truscott, Cavitation of a submerged jet, Exp. Fluids 54 (2013) 1541.

[34] E. Hutli, M.S. Nedeljkovicc, N.A. Radovic, A. Bonyár, The relation between the high speed submerged cavitating jet behaviour and the cavitation erosion process, Int. J. Multiph. Flow 83 (2016) 27–38.

[35] W. Lauterborn, Kavitation Durch Laserlicht, Acustica 31 (1974) 51–78.

[36] E.A. Brujan, K. Nahen, P. Schmidt, A. Vogel, Dynamics of Laser-Induced Cavitation Bubbles Near an Elastic Boundary, J. Fluid Mech. 433 (2001) 251–281.

[37] A. Karimi, J.L. Martin, Cavitation erosion of materials, Int. Met. Rev. 31 (1986) 1–26.

[38] H. Kim, T. Negishi, M. Kudo, H. Takei, K. Yasuda, Quantitative backscattered electron imaging of the field emission scanning electron microscopy for discrimination of the nanoscale elements with nm order spatial resolution, J. Electron Microscopy 59 (2010) 379–385.

[39] T.N. Angelidis, S.A. Sklavounos, A SEM-EDS study of new and used automotive catalysts, Appl. Catal. A 133 (1995) 121–132.

[40] D.M. Aruguete, M. Murayama, T. Blakney, C. Winkler, Enhanced release of palladium and platinum from catalytic converter materials exposed to ammonia and chloride bearing solutions, Environ. Sci.: Processes Impacts 21 (2019) 133–144.

[41] C. Fontas, V. Salvado, M. Hidalgo, Separation and Concentration of Pd, Pt, and Rh from Automotive Catalytic Converters by Combining Two Hollow-Fiber Liquid Membrane Systems, Ind. Eng. Chem. Res. 41 (2002) 1616–1620.

[42] J. Faber, K. Brodzik, Influence of preparation and analysis methods on determination of Rh, Pd and Pt content in automotive catalysts samples, IOP Conf. Ser.: Mater. Sci. Eng. 421 (2018), 042018.

[43] I. Yakoumis, A.M. Moschovi, I. Giannopoulou, D. Panias, Real life experimental determination of platinum group metals content in automotive catalytic converters, IOP Conf. Ser.: Mater. Sci. Eng. 329 (2018), 012009.

[44] Thermo Fisher Scientific - Elemental Analyzers and Phase Analyzers. Determination of Precious Metal Content in Catalytic Converters. AZoM, 2019 viewed 07 February 2020, https://www.azom.com/article.aspx?ArticleID=5993.

[45] S. Cherevko, A.R. Zeradjanin, A.A. Topalov, N. Kulyk, I. Katsounaros, K.J. Mayrhofer, Dissolution of Noble Metals during Oxygen Evolution in Acidic Media, ChemCatChem 6 (2014) 2219–2223.

[46] C. Noergaard, S. Stamatin, E. Skou, Redeposition of electrochemically dissolved platinum as nanoparticles on carbon, Int. J. Hydrogen Energy 39 (2014) 17322–17326.

[47] B. Swain, J. Jeong, S. Kim, J. Lee, Separation of platinum and palladium from chloride solution by solvent extraction using Alamine 300, Hydrometallurgy 104 (2010) 1–7.

[48] A. Ciocanea, E. Vasile, V. Ionescu, F.I. Maxim, C. Diac, C. Miron, SN Stamatin Second Life Application of Automotive Catalysts: Hydrodynamic Cavitation Recovery and Photo Water Splitting, Metals 10 (2020) 1307.

[49] J.Y. Lee, B. Raju, B.N. Kumar, J.R. Kumar, H.K. Park, B.R. Reddy, Solvent extraction separation and recovery of palladium and platinum from chloride leach liquors of spent automobile catalyst, Sep. Purif. Technol. 73 (2010) 213–218.

[50] B. Gupta, I. Singh, Extraction and separation of platinum, palladium and rhodium using Cyanex 923 and their recovery from real samples, Hydrometallurgy 134–135 (2013) 11–18.